

OPTIMISATION OF JOINTS BETWEEN SUPERCONDUCTING  
 $\text{Bi}_2\text{Sr}_2\text{CaCu}_2\text{O}_{8+\delta}$  AND Ag CURRENT LEADS

A. KURŠUMOVIĆ and J. E. EVETTS

*IRC in Superconductivity and Department of Materials Science, University of  
Cambridge, Cambridge CB2 3QZ, UK.*

**Dedicated to Professor Boran Leontić on the occasion of his 70<sup>th</sup> birthday**

Received 14 February 2000; Accepted 10 April 2000

Electric contacts, for high current applications, between  $\text{Bi}_2\text{Sr}_2\text{CaCu}_2\text{O}_{8+\delta}$  superconductor and thick Ag tapes were in-situ processed during partial melting and texturing of the superconductor. At currents,  $I$ , below the critical current,  $I_C$ , a constant joint resistance,  $R_C$ , appears. Prolonged high-temperature annealing of current elements that produces samples of higher texture and higher  $I_C$  showed a correspondingly lower  $R_C$  hence lower power dissipation, due to lower contact resistivity ( $\rho_C \approx 55 \times 10^{-9} \Omega\text{cm}^2$  at 77 K). Increasing the silver thickness further decreases power dissipation at joint. Current transfer occurs on a 1 mm scale in this regime. At higher currents ( $I > I_C$ ), non-ohmic behaviour is observed. At very high currents ( $I \approx 10 I_C$ ) the flux flow resistance of the superconducting element becomes comparable to the resistance of the Ag part in the joint, resulting in current sharing, approaching a rather uniform current distribution over the whole contact. This eventually reduces power dissipation in the contact to a value below that of the superconductor itself, reducing the possibility of element failure at the contact.

PACS numbers: 74.25.F, 81.40.R

UDC 538.945

Keywords:  $\text{Bi}_2\text{Sr}_2\text{CaCu}_2\text{O}_{8+\delta}$  superconductor, electric contacts, joint resistance, very high currents

## 1. Introduction

Superconductors in most applications require normal metal power leads to be connected to an electricity network. The quality of this metal-superconductor joint is of great importance and should have a design specification adequate to assure trouble free operation (i.e. no quenching of the superconductor in the contact zone).

Any non-uniformity in the contact can result in hot spot formation that can lead to localised thermal quenching and destruction of the contact due to much increased power dissipation. In addition a large contact resistance results in excessive loss of liquid nitrogen during normal operation while superconductors have “zero” resistivity since they carry a current ( $I$ ) below the critical current ( $I_C$ ). However, in some applications such as fault current limiters [1] AC currents many times higher than the critical current are experienced. In this regime the flux flow resistivity of the ceramic superconductor in short periods of time becomes comparable to the resistivity of the metallic current lead [2] creating new requirements on the contact.

However, making a low resistance and robust connection for ceramic superconductors to a metal lead, that can withstand electrical, thermal and mechanical shocks, presents a demanding task. In HTS superconductors, such as Bi-2212, texturing produces highly aligned microstructures [3,4], increasing transport properties, especially the critical current density. The grain alignment should in principle influence the apparent contact resistivity or more precisely contact resistance of in-situ made contacts. Hence, in this study, texturing of  $\text{Bi}_2\text{Sr}_2\text{CaCu}_2\text{O}_8$  (Bi-2212) and joint geometry influence on current transfer, at current joints between Ag and Bi-2212 were investigated for currents from  $I < I_C$  to currents as high as  $10 I_C$ .

## 2. Experimental

Composite reaction texturing (CRT) [3,4] is based on texturing of  $\text{Bi}_2\text{Sr}_2\text{CaCu}_2\text{O}_8$  (Bi-2212) phase on uniaxially aligned MgO single crystal fibres in the Bi-2212 matrix. The nucleation of the Bi-2212 phase of a right orientation, with the superconducting ab-planes aligned with the fibre axes, occurs during solidification of partially molten matrix leading to a highly textured microstructure with the superconducting ab-planes aligned with the fibre axes [4]. In this work, the MgO fibres were made in-house while Bi-2212 powder was supplied by MERCK. Flat Ag current leads for in-situ contacts are inserted into the green laminate parallel to the expected ab-plane. About 5wt.% Ag-powder is added to the original Bi-2212 precursor, in order to avoid contact dissolution during melt processing.

A new batch of samples was prepared complementary to the two batches made earlier whose results were reported elsewhere [2]. The samples were about 5 mm wide, 1.4 mm thick and 60 mm long. This batch was processed 240 h in the grain growth regime that is much longer time than usual (10 h), resulting in a higher critical current density [2]. Samples were made with in-situ processed 0.125 mm thick silver tapes (current leads) of the same width (about 5 mm) as the superconducting element. However, one sample was made with a 0.25 mm thick silver lead. They were all embedded about 10 mm into the superconductor (see Fig. 1).

Electrical measurements at the contact and along the sample were performed by a standard four-probe method measuring the voltage drop over whole contact (Fig. 1), while passing a controlled current through the silver-current lead. Voltage contacts were made with 25  $\mu\text{m}$  silver wires. The  $E - I$  characteristic of the superconductor was also monitored remote from the contact. The current sources used were a Hewlett Packard HP6680A supply (870 A, DC) and a custom built pro-

grammable 50 Hz supply (about 3000 A, AC). This power supply allowed pulses of one up to 200 AC half cycles to be applied. The critical current was defined at  $10^{-6}$  Vcm $^{-1}$  electric field.

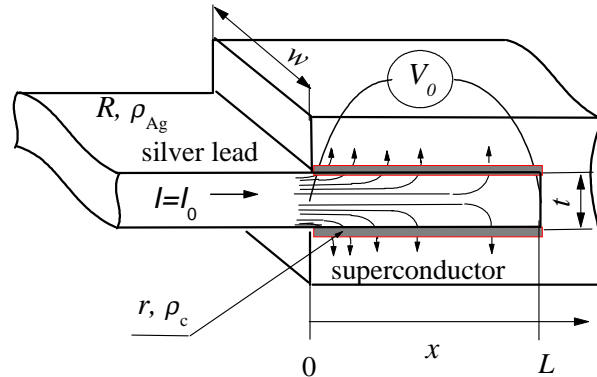


Fig. 1. Joint configuration and visualisation of current flow between the metal and the superconductor used for in-situ processed contacts for measurements of cumulative voltage drop ( $V_0$ ) at the contact while passing a transport current  $I_0$ . The silver current lead has thickness  $t$ , while the superconductor is 5 to 10 times thicker. The width  $w$  of both silver and superconductor were made the same.

### 3. Results

In Fig. 2 the total voltage drop,  $V_0$ , across the current joint for a sample of higher critical current density ( $J_C \approx 1800$  Acm $^{-2}$ ) prepared in this work and for samples of lower critical current density ( $J_C \approx 750 - 1500$  Acm $^{-2}$ ) [2] are shown. The  $E - I$  characteristics for the corresponding superconductors are also shown. As shown earlier [2],  $V_0$  is linear with  $I_0$  at low currents ( $I < I_C$ ), while at high currents ( $I \geq I_C$ ),  $V_0$  deviates from linear behaviour. As can be seen, the voltage drop across the joint decreases with increasing critical current density of the samples, i.e. by prolonged annealing as a result of higher degree of texturing (Fig. 2).

Figure 3 shows the comparison of the voltage drop,  $V_0$ , at normal metal-superconductor joints on the same sample made with 0.125 and 0.250 mm thick Ag current leads. The  $V_0 - I$  behaviour shows lower voltage drop across the joint but similar overall features as in the case of thinner Ag-lead.

The voltage drop at contact for high current pulsing (sample of ( $J_C \approx 1500$  Acm $^{-2}$ ) is shown in Fig. 4. The  $E - I$  behaviour of the superconductor and voltage drop across 1 cm long silver lead is also shown in Fig 4. The sudden increase in the field ( $E$ ) of the superconductor at very high currents (about  $13 I_C$ ) occurs due to the quenching when the sample goes into a resistive state resulting in current limiting like in fault current limiter applications [1]. Prior to this regime, the voltage drop along 1 cm joint becomes lower than electric field in the superconductor. There were no sign of adverse effects on the metal-superconductor joint from high current

pulsing, showing good reproducibility over the course of the experiment (about 20 separate measurements).

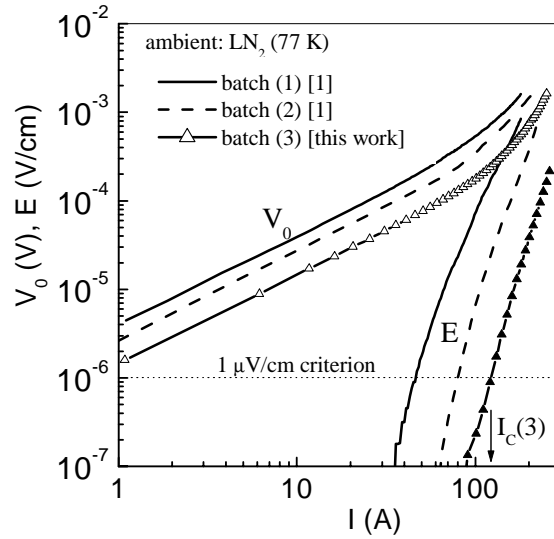


Fig. 2. Self-field  $E - I$  characteristics for the superconductor and the voltage drop,  $V_0$ , across the superconductor-metal joint, for samples from Ref. [2] and this work, showing gradual contact improvement with texturing. In all cases silver leads were 0.125 mm thick tapes.

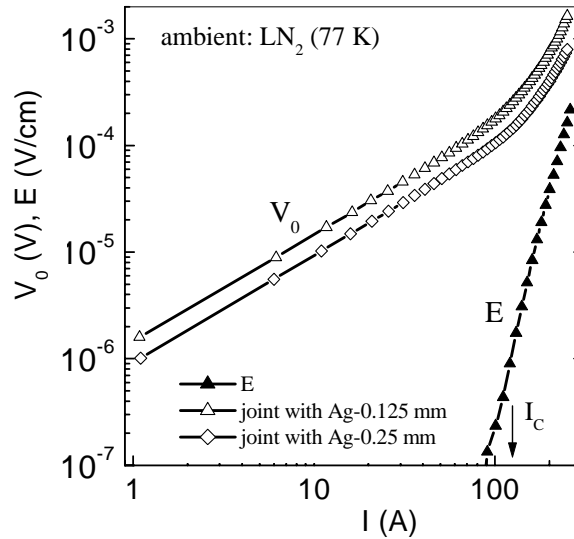


Fig. 3. Self-field  $E - I$  characteristics for the superconductor and the voltage drop,  $V_0$ , across the superconductor-metal joint, for joints with 0.125 and 0.25 mm thick silver leads.

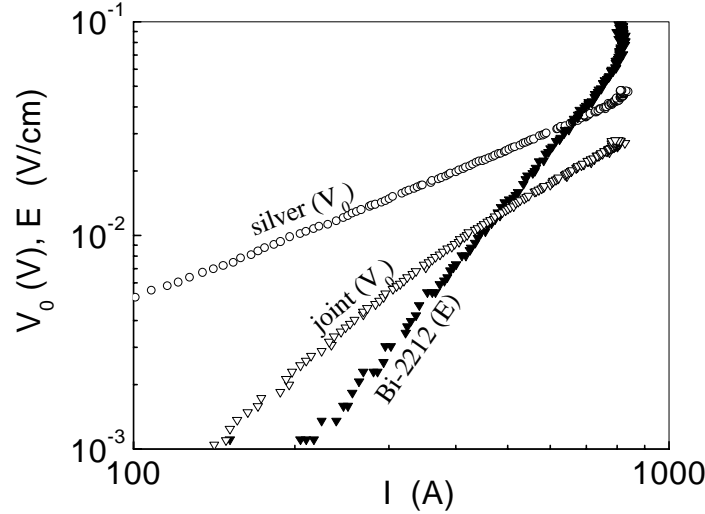


Fig. 4.  $V - I$  characteristics for a 1 cm long joint and separately for the superconductor and Ag parts of the same length at very high currents measured during nearly adiabatic high current pulsing (5 ms duration).

## 4. Analysis

### 4.1. Low current case

Planar contacts between metals and superconductors at power engineering frequencies (50-440 Hz), are regarded as pure ohmic. A transmission line model is often used in describing metal-superconductor [2,5] and metal-semiconductor [6] contacts. The current joint is seen as a transmission line of length  $L$  in the  $x$  direction (Fig. 1) with the line resistance  $R$  (Ag here) per unit length [ $\Omega/\text{cm}$ ] and  $G$  the contact conductance per unit length [ $1/(\Omega\text{cm})$ ]. The term  $G$  is related to the contact resistivity per unit length,  $r = 1/G$ . The transmission line model for the potential  $V(x)$  and current  $I(x)$  can be applied yielding the solution [2,5]

$$V(x) = I_0 \sqrt{Rr} \frac{e^{(x-L)/L_T} + e^{-(x-L)/L_T}}{e^{L/L_T} - e^{-L/L_T}} = I_0 \sqrt{Rr} \frac{\text{ch}[(x-L)/L_T]}{\text{sh}(L/L_T)}, \quad 0 < x < L. \quad (1)$$

$I = I_0$  is the total current (Fig. 1) and  $L_T = \sqrt{r/R}$  is the transfer length over which almost all of current is transferred from the normal metal (resistive current lead) to the superconductor. The transfer length corresponds to the inverse of the attenuation factor in a transmission line. The joint resistance (in  $\Omega$ ) and power dissipation (in W) are:  $R_C = V_0/I_0 = \sqrt{Rr} \text{cth}(L/L_T) = RL_T \text{cth}(L/L_T)$ ,  $P = V_0 I_0 = I_0^2 \sqrt{Rr} \text{cth}(L/L_T) = I_0^2 RL_T \text{cth}(L/L_T)$ , where  $V_0$  is the total voltage drop along the joint. There are two extreme solutions for  $R_C$  and  $P$  [2,5]. For short joints where  $L \ll L_T$ ,  $\text{cth}(L/L_T) \approx (L/L_T)^{-1}$ , joint resistance and power dissipation are  $R_C \approx 1/(L/r)$ , and  $P \approx I_0^2/(L/r)$ , respectively. Thus for relatively short contacts,

power dissipation increases as  $1/L$  as the length of the current joint becomes shorter. However, there is no real situation here and it is important only in semiconductors. For joints long enough where  $L \gg L_T$  and  $\text{cth}(L/L_T) \approx 1$ , joint resistance and power dissipation become:

$$\text{and} \quad R_C \approx \sqrt{Rr}, \quad (2)$$

$$P \approx I_0^2 \sqrt{Rr}, \quad (3)$$

which is reasonably well fulfilled for  $L > 2L_T$  [2,5]. Further increasing the contact length  $L$  neither significantly decreases the resistance nor the power dissipation.

The contact resistivity ( $\rho_C$ ) is calculated from (2). In the contact configuration used (Fig. 1), the central plane of the silver lead is a mirror plane of symmetry. Therefore, all results for the transmission line model [2] apply (with  $r \approx R_C^2/R = \rho_C/2w$  and  $R = \rho_{Ag}/wt$ ) giving

$$\rho_C = (2wR_C)^2 t / (2\rho_{Ag}). \quad (4)$$

The transfer length is easily calculable for the present geometry as

$$L_T \approx \sqrt{r/R} = \sqrt{\frac{\rho_C/2w}{\rho_{Ag}/wt}} = \sqrt{\frac{\rho_C t}{2\rho_{Ag}}}. \quad (5)$$

The results are summarised in Table 1. As can be seen, the joint resistance (taken from Figs. 2 and 3) decreases with increasing critical current, i.e. texturing of the current elements. This directly reduces power dissipation at the joint. This is a result of increased contact quality, i.e. decreased contact resistivity (from  $0.26 \mu\Omega\text{cm}$ ) around five times (to  $\rho_C$  of  $0.055 \mu\Omega\text{cm}$ ) after long annealing. At the same time, the current transfer length,  $L_T$ , decreases with increasing contact resistivity to a half of the original size, from  $0.75$  to  $0.35$  mm in the case of  $0.125$  mm thick Ag lead. Intensified current crowding is expected with shortening the transfer length, but power dissipation remains apparently unaffected by this due to lower contact

TABLE 1. Comparative results for samples of different critical current densities and with different Ag-lead thickness.

Batch	$t/\text{Ag}$ (mm)	$J_C$ ( $\text{Acm}^{-2}$ )	$R_C$ ( $\mu\Omega\text{cm}$ )	$\rho_C$ (mW)	$L_T$ (mm)	Ref.
1	0.125	750	3.5	0.260	0.75	[1]
2	0.125	1500	2.7	0.165	0.60	[1]
3 (a)	0.125	1800	1.6	0.055	0.35	This work
3 (b)	0.250	1800	1.2	0.062	0.50	This work

resistivity. Furthermore, the joint resistance in the case of a  $0.250$  mm thick Ag lead is about  $1.2 \mu\Omega$ , that is about  $\sqrt{2}$  times lower than of the  $0.125$  mm Ag joint, as expected from Eq. (4), thus a thicker normal metal part can be used to reduce further overall power loss at the joint.

#### 4.2. High current case

In the high current applications ( $I \gg I_C$ ), a more complicated approach is needed for full description of the nature of power dissipation at the joint. Numerical modelling was found more convenient than an analytical approach [2,7]. However, the number of parameters, such as noticeable resistance of the superconductor, anisotropy as well as local heating, play a role. It was observed that current sharing takes place to a great extent resulting in an almost linear current transfer across the joint [2]. This can be also concluded from Fig. 5. It is obvious (Fig. 5) that the resistance of the superconductor in the joint becomes comparable and higher than the silver part in the configuration used (Bi-2212 was made about ten times thicker than Ag) resulting in correspondingly lower joint resistance than both of them. This makes possible working at very high currents without a risk of contact failure. However, superconductors with higher critical current densities show somewhat lower resistivity (and resistance) in the flux-flow regime near the “current quenching”, therefore, accordingly thicker silver leads should be used.

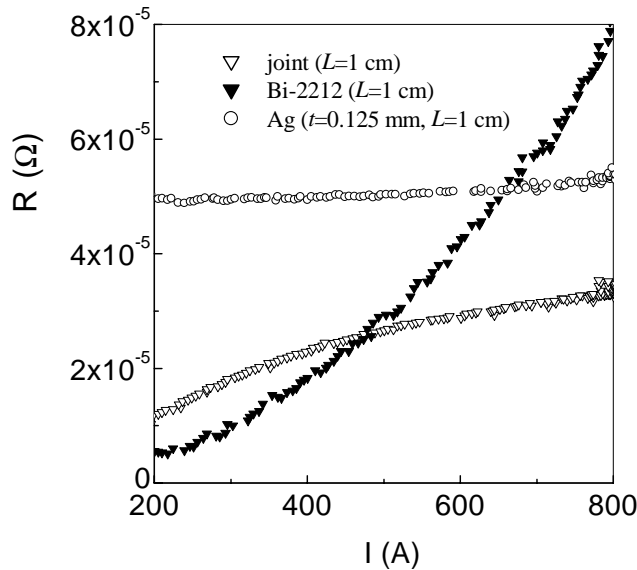


Fig. 5. Resistance of a 1 cm long joint compared with the resistances of the superconductor and Ag lead of the same length measured at very high currents ( $I > 10 I_C$ ), during nearly adiabatic current pulsing (5 ms duration).

Figure 6 shows power dissipation ( $P$ ) over the whole range of currents for samples of different current densities. As can be seen for in-situ contacts,  $P$  is reduced by an order of magnitude after prolonged annealing and using thicker silver leads, for currents below the critical current (about 100 A here). For higher currents ( $I \gg I_C$ ), the contact resistivity becomes less important, hence only resistance of the silver lead and flux flow resistivity of the superconductor in the joint contribute to the power dissipation. Therefore, the joint resistance and hence the

power dissipation of the joint become dependent on the resistive properties of the superconductor as well.

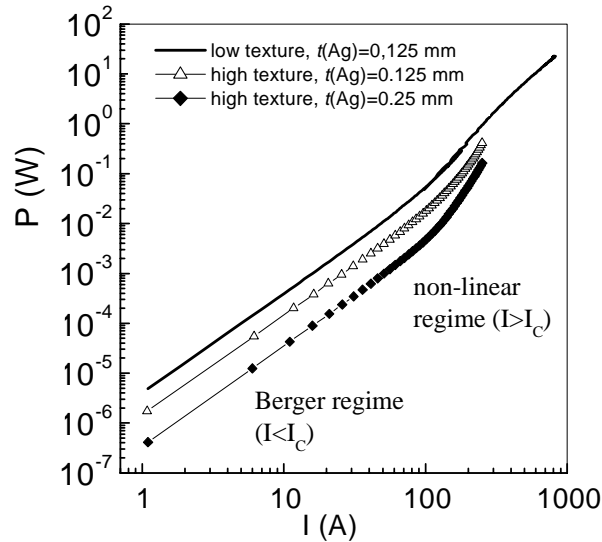


Fig. 6. Power dissipation,  $P = V_0 I_0 = R_C I_0^2$ , in both measuring regimes (DC and AC) for different annealing conditions and different silver lead thicknesses (see Figs. 2 and 3).

## 5. Discussion

As found earlier [2], at low currents ( $I < I_C$ ) and in self-field,  $V_0$  is linear with  $I$ , i.e. contact resistance is constant. The power dissipation exhibits simple power law behaviour ( $P \propto I^2$ ) for  $I < I_C$ . This suggests that a simple transmission line model is strictly applicable for usual operating conditions ( $I < I_C$ ). This model allows the calculation of contact resistivity from the measured joint resistance and known Ag lead resistance.

Power dissipation (3) at the metal-superconductor joint occurs by both the resistance of metal part and the resistance of the interfacial layer (contact). Minimisation of the joint resistance (2) is necessary in order to minimise power dissipation (3). Therefore, both the resistance of metallic part and the contact resistivity should be minimised. The easiest way is to increase thickness ( $t$ ) of the silver lead that reduces joint resistance and power dissipation proportional to  $\sqrt{t}$ . For the case of silver part, there are some processing and exploitation limitations to the increasing thickness. However, the Ag thickness used in this study ( $t = 0.125$  and  $0.25$  mm) did not invoke any problems, and contacts stayed electrically and mechanically stable after long use involving abrupt immersing of samples into a liquid nitrogen bath, followed by rapid heating to the room temperature.

Significant improvement of the contact conductivity can be achieved by prolonged annealing in the grain-growth regime, increasing the critical current density, resulting in the contact resistivity drop from  $0.26 \mu\Omega\text{cm}$  for material with lower  $J_C$ , to  $0.055 \mu\Omega\text{cm}$  for the material with highest  $J_C$ . This is a rather significant decrease in the contact resistivity, comparing favourably with the results published so far for in-situ and ex-situ processing of Ag/Bi-2212 contacts [2,8,9]. The decrease in the estimated contact resistivity is believed to be mainly due to the increased Bi-2212 texture at the superconductor-silver interface, maximising the surface area for current transfer between Bi-2212 grains and silver. It is known that also the interface contamination can severely deteriorate contact quality [9], hence decrease in contact resistivity could be partly due to the refinement of the superconductor structure and the interface between silver lead and Bi-2212.

Contact resistivity ( $\rho_C$ ), estimated by the transmission line model, appears to deviate significantly from the true contact resistance  $\rho_0$ , increasing nonlinearly above  $I_C$ . This is a direct consequence of the local flux-flow resistance in the superconductor in the zone of the current transfer, where locally the current significantly exceeds the critical current density. However, strong anisotropy in the superconductor results in a much lower  $I_C$  value and higher flux-flow resistivity in the c-axis direction and is believed to contribute considerably to this behaviour [7]. As a result, flux flow makes a measurable contribution to the joint resistance. This means that a simple transmission-line model is no longer strictly applicable. However, the current transfer length increased progressively over the whole contact [2].

Power dissipation at very high currents becomes less dependent on the true contact resistivity and much more on the resistance of the metal and superconducting (flux-flow) parts in the joint. It is shown here that in that region superconductor part in the joint becomes easily more resistive (even prior going to full normal state) than the metal lead. In the case when flux-flow resistance becomes comparable to the resistance of the silver lead, a nearly linear transfer occurs along the length of the current joint [2] making nucleation of a normal zone on the contact area less likely.

## 6. Conclusions

The linear model [10] has been found to apply well for normal operating currents,  $I_0 < I_C$ , where contact resistivity shows ohmic behaviour, allowing a strict application of the transmission-line model. Very wide range of contact resistivity is found,  $R_C = 0.05$  to  $0.26 \mu\Omega\text{cm}^2$ , decreasing with increasing texturing for in-situ made contacts.

The apparent contact resistivity significantly increases above  $I_C$ , having an additional contribution due to the flux flow of the superconductor. At very high currents, resistance of the superconductor becomes comparable and even higher than of the normal metal lead current sharing takes place over a large portion of the contact since contact resistance becomes negligible. In this regime, nucleation of a normal zone on the contact area is less likely than in the superconductor itself.

*Acknowledgements*

The work was supported under an EPSRC LINK project, and the European Union TMR Network SUPERCURRENT.

## References

- [1] A. Kuršumović, B. A. Glowacki, J. E. Evetts, M. Chen, M. A. Henson, M. P. Hills and R. M. Henson, *Applied Superconductivity 1999 (EUCAS 1999)*, Inst. Phys. Conf. Ser. in press; A. T. Rowley, F. C. R. Wroe, M. P. Saravolac, K. Tekletsadik, J. Hencox, D. Watson, J. E. Evetts, A. Kuršumović and A.M. Campbell, *Applied Superconductivity (1997)*, Inst. Phys. Conf. Ser. No 158, 1235 (1997).
- [2] A. Kuršumović, R. P. Baranowski, B. A. Glowacki and J. E. Evetts, *J. Appl. Phys.* **86** (1999) 1569.
- [3] D. R. Watson and J. E. Evetts, *Supercond. Sci. Technol.* **9** (1996) 327; D. R. Watson M. Chen and J. E. Evetts, *Supercond. Sci. Technol.* **8** (1995) 311.
- [4] M. Chen, D. M. Glowacka, B. Soyly, D. R. Watson, J. K. S. Christiansen, R. P. Baranowski, B. A. Glowacki and J. E. Evetts, *IEEE Trans. on Applied Superconductivity* **5** (1995) 801.
- [5] M. N. Wilson, in *Monographs on Cryogenics 2: Superconducting Magnets*, Clarendon Press, Oxford (1983).
- [6] M. Shur, *Microdevice Physics and Fabrication Technologies: GaAs Devices and Circuits*, Plenum Press, New York (1987) Ch. 3.
- [7] R. P. Baranowski, A. Kuršumović and J. E. Evetts, *Applied Superconductivity 1999 (EUCAS 1999)*, Inst. Phys. Conf. Ser., in press.
- [8] E. Preisler, J. Bayersdrfer, M. Brunner, J. Bock and S. Elschner, *Supercond. Sci. Technol.* **7** (1994) 389.
- [9] H. Imao, S. Kishida and H. Tokutaka, *Jpn. J. Appl. Phys.* **35** (1996) 5299.
- [10] H. H. Berger, *Sol. St. Electronics* **15** (1972) 145.

OPTIMIZACIJA SPOJEVA SUPRAVODLJIVOG  $\text{Bi}_2\text{Sr}_2\text{CaCu}_2\text{O}_{8+\delta}$  I Ag

Obrađivali smo jakostrujne električne spojeve supravodiča  $\text{Bi}_2\text{Sr}_2\text{CaCu}_2\text{O}_{8+\delta}$  i debelih vrpca Ag djelomičnim talenjem i prožimanjem spoja. Za struje  $I$  manje od kritične struje,  $I_C$ , pojavljuje se stalan otpor spoja,  $R_C$ . Produljeno napuštanje strujnih elemenata na visokoj temperaturi, koje daje uzorke s većim prožimanjem i višim  $I_C$ , pokazuje skladno tome manji  $R_C$  i stoga manje gubitke, zbog manje otpornosti spoja ( $\rho_C \approx 55 \times 10^{-9} \Omega\text{cm}^2$  pri 77 K). Povećanje debljine uzrokuje daljnje smanjenje gubitaka u spoju. U tim se uvjetima struja prenosi u sloju debljine oko 1 mm. Za jače struje ( $I > I_C$ ) opaža se neomska ovisnost. Za vrlo jake struje ( $I \approx 10 I_C$ ), otpor zbog selenja silnica postaje usporediv otporu srebrnog dijela spoja, što vodi na dijeljenje struje te se postiže vrlo jednolika raspodjela struje preko cijelog spoja. To smanjuje gubitke u spoju na vrijednost manju od one u samom supravodiču i smanjuje mogućnost zatajivanja rada spoja.